Supporting Information

Ratiometric fluorescence chemosensor based on Tyrosine derivatives for monitoring mercury ions in aqueous solutions

Ponnaboina Thirupathi, Ponnaboina Saritha (née Gudelli) and Keun–Hyeung Lee*

Bioorganic Chemistry Laboratory, Center for Design and Applications of Molecular Catalysts, Department of Chemistry and Chemical Engineering,

Inha University, 253 Yonghyun–Dong, Nam–Gu, Incheon, 402–751, Korea

Email: leekh@inha.ac.kr (K.-H. Lee)

Contents

1. Figures

1. Figures

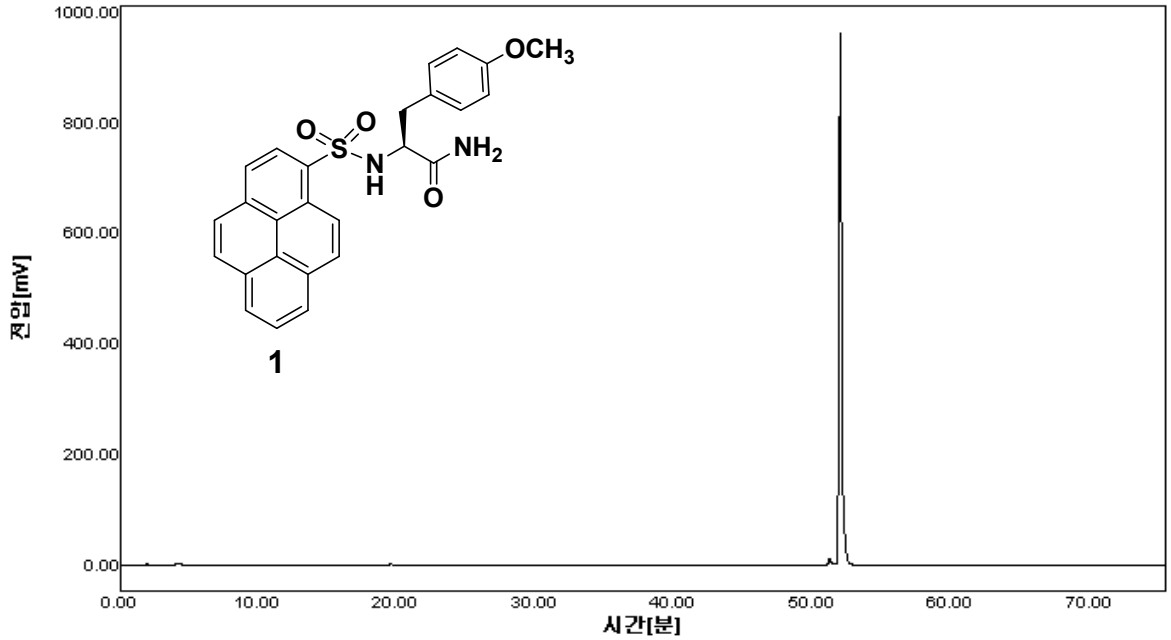

Fig. S1 HPLC chromatogram of compound **1**

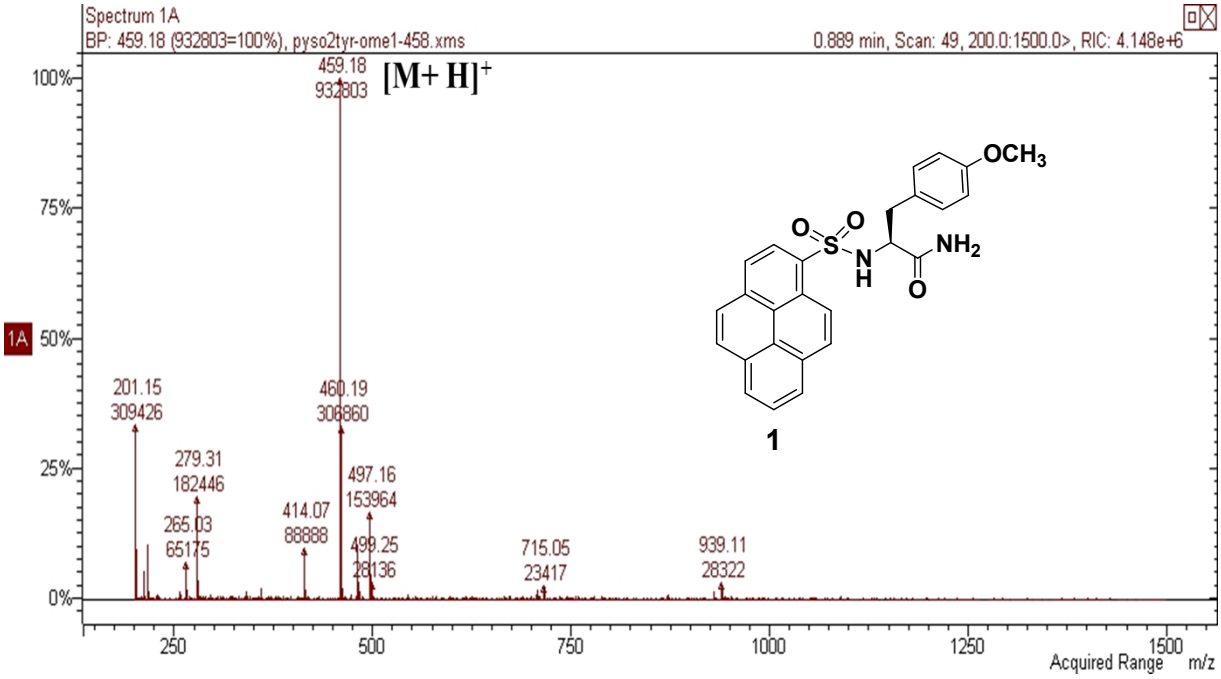

Fig. S2 ESI mass spectrum of **1**

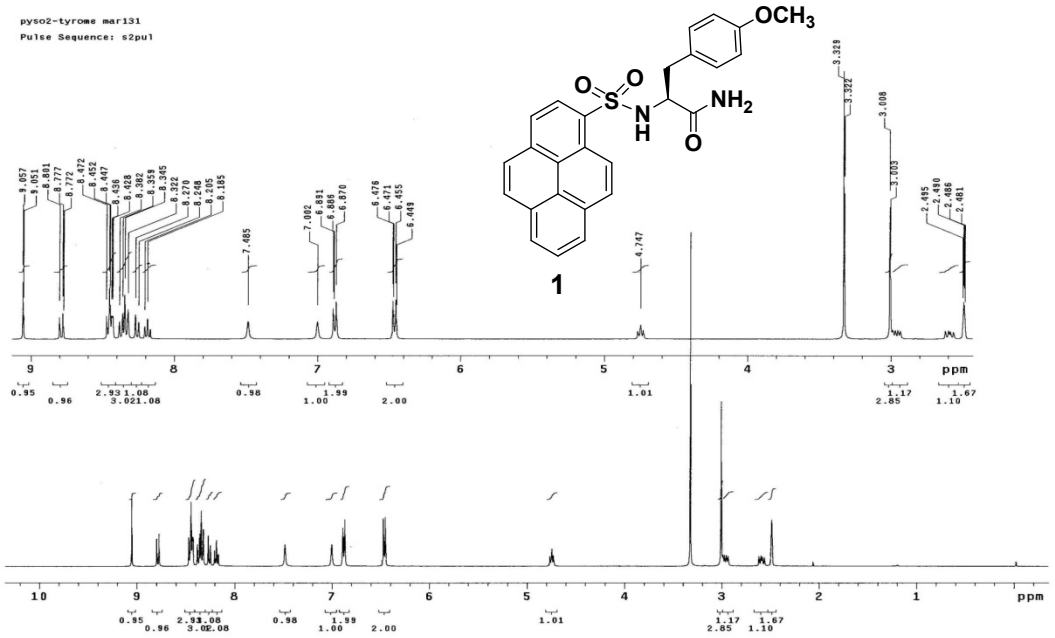

Fig. S3 ^{1}H NMR spectrum of compound **1**

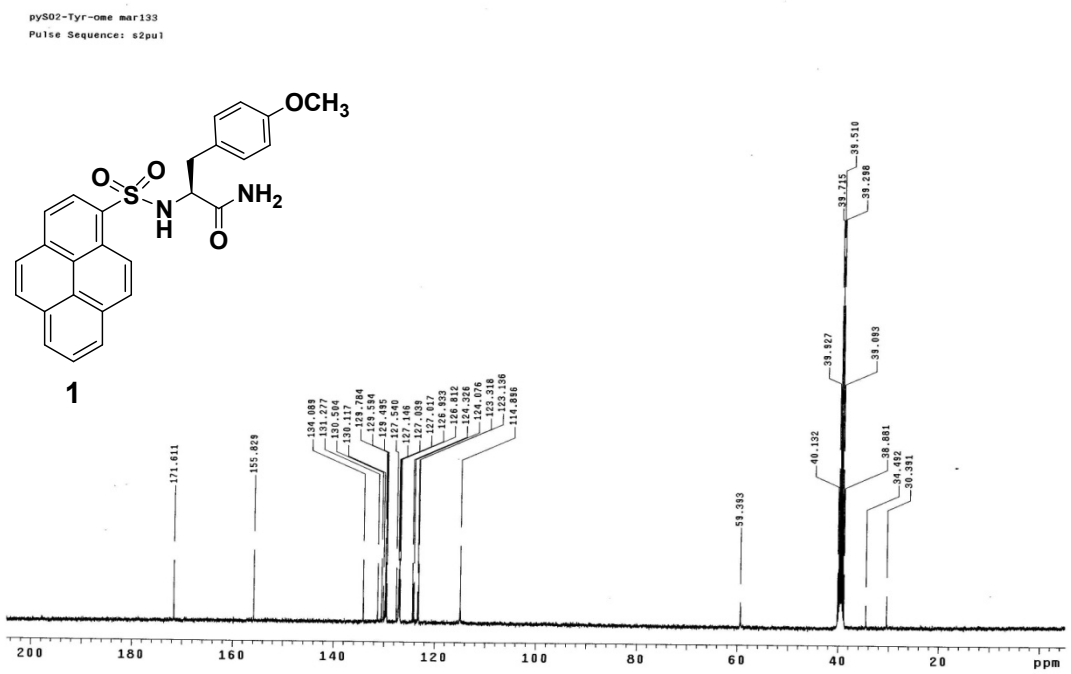

Fig. S4 ^{13}C NMR spectrum of compound **1**

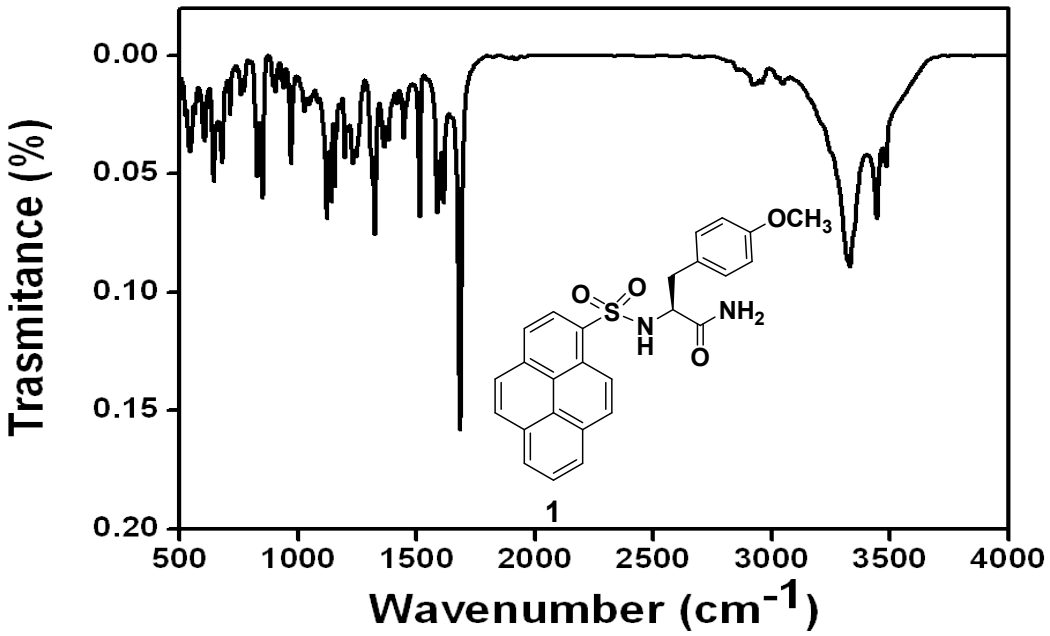

Fig. S5 IR spectrum of **1**

1) PYSO2-1 *with GLY (POS)*

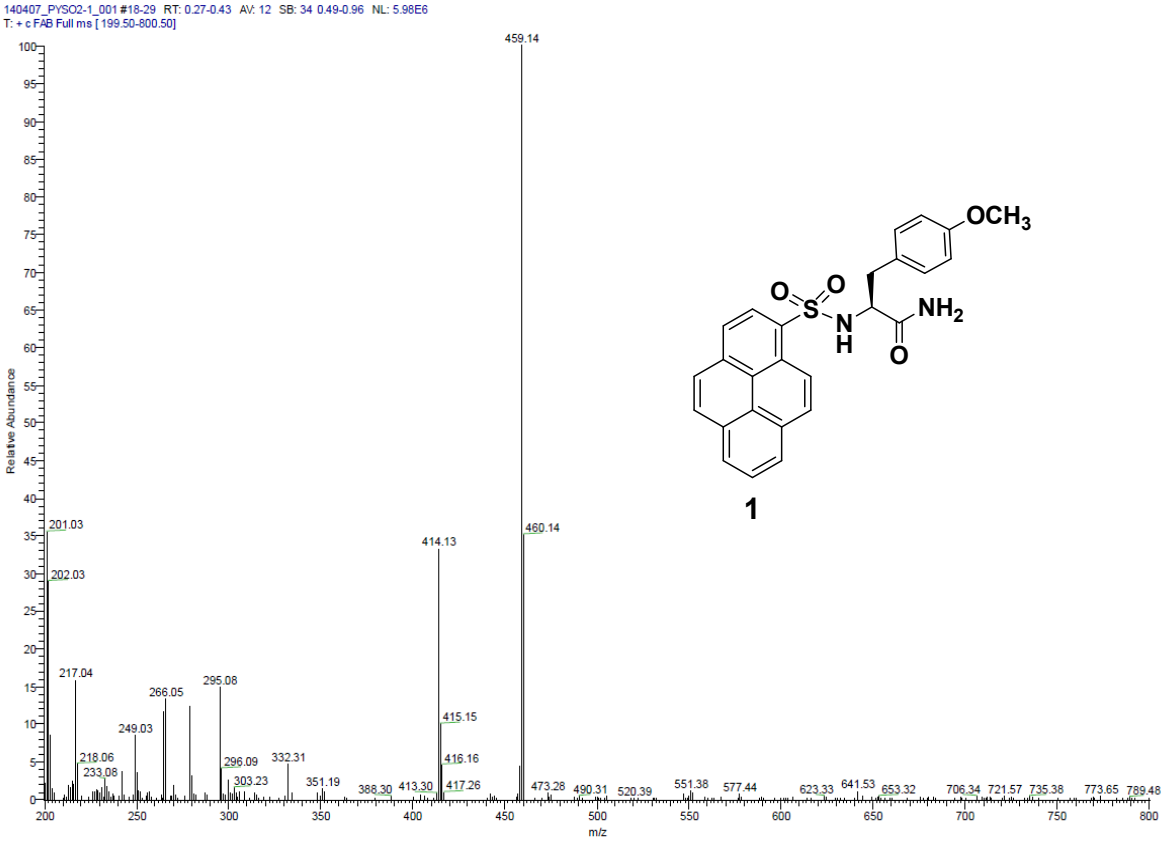

Fig. S6 HRMS-FAB mass spectrum of **1**

1) PYSO2-1 *with GLY (POS)*

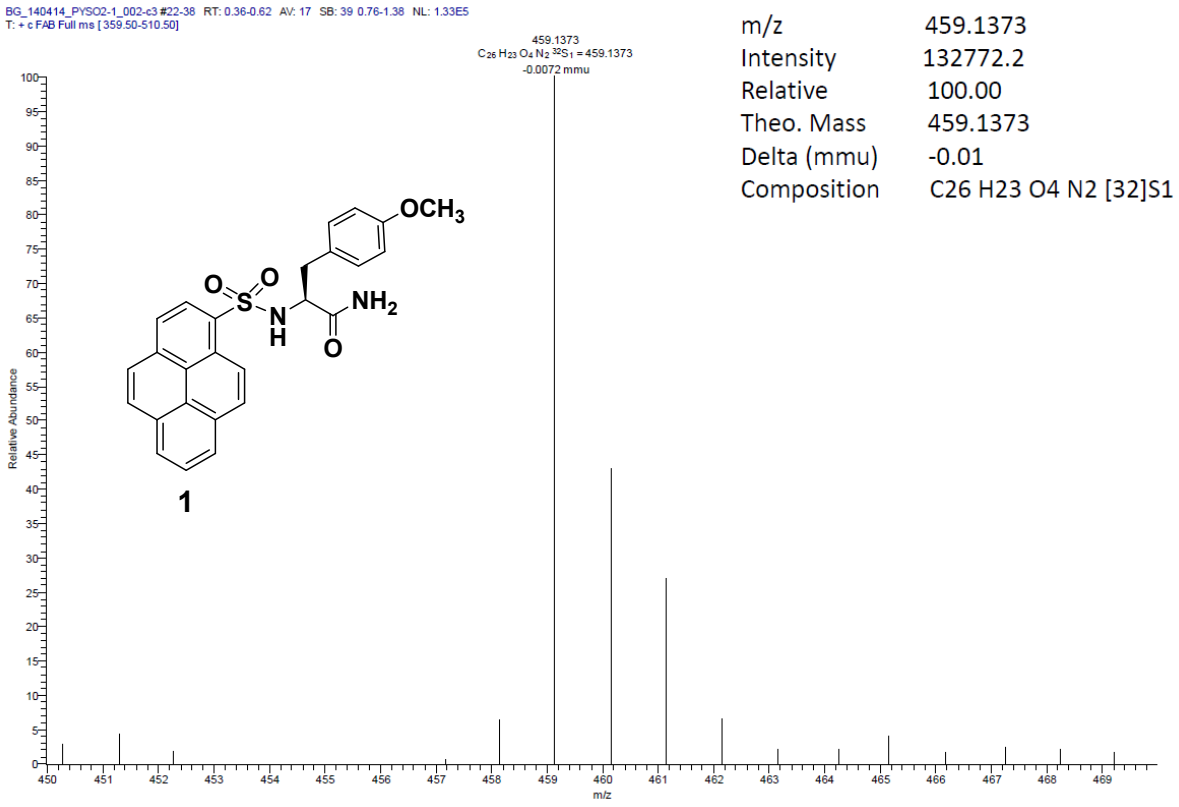

Fig. S7 HRMS-FAB elemental composition of **1**

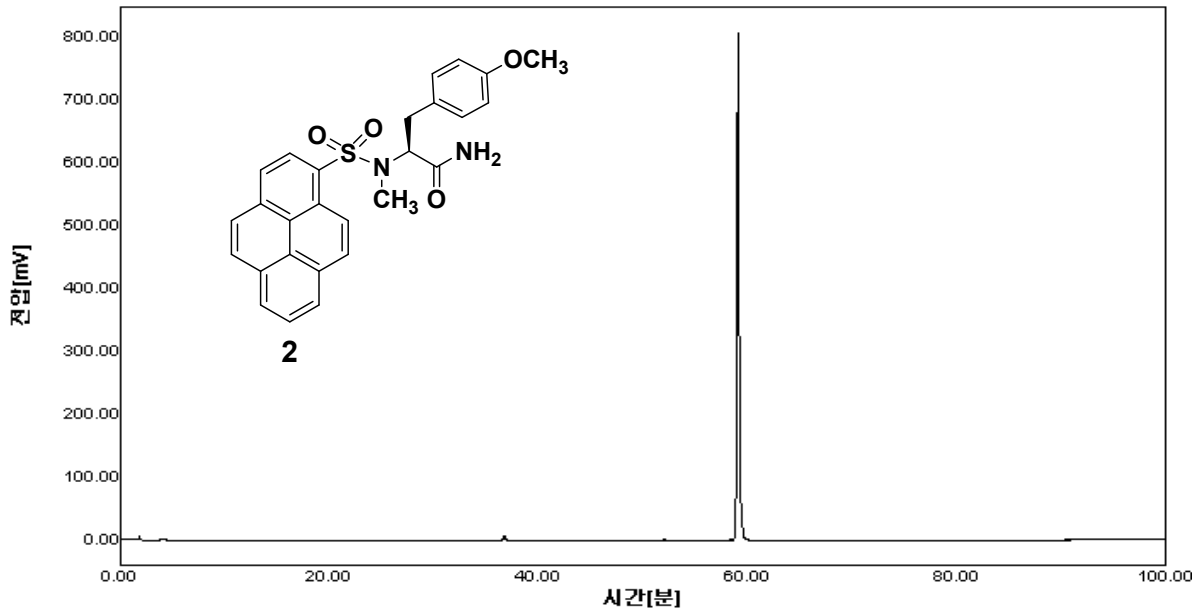

Fig. S8 HPLC chromatogram of compound **2**

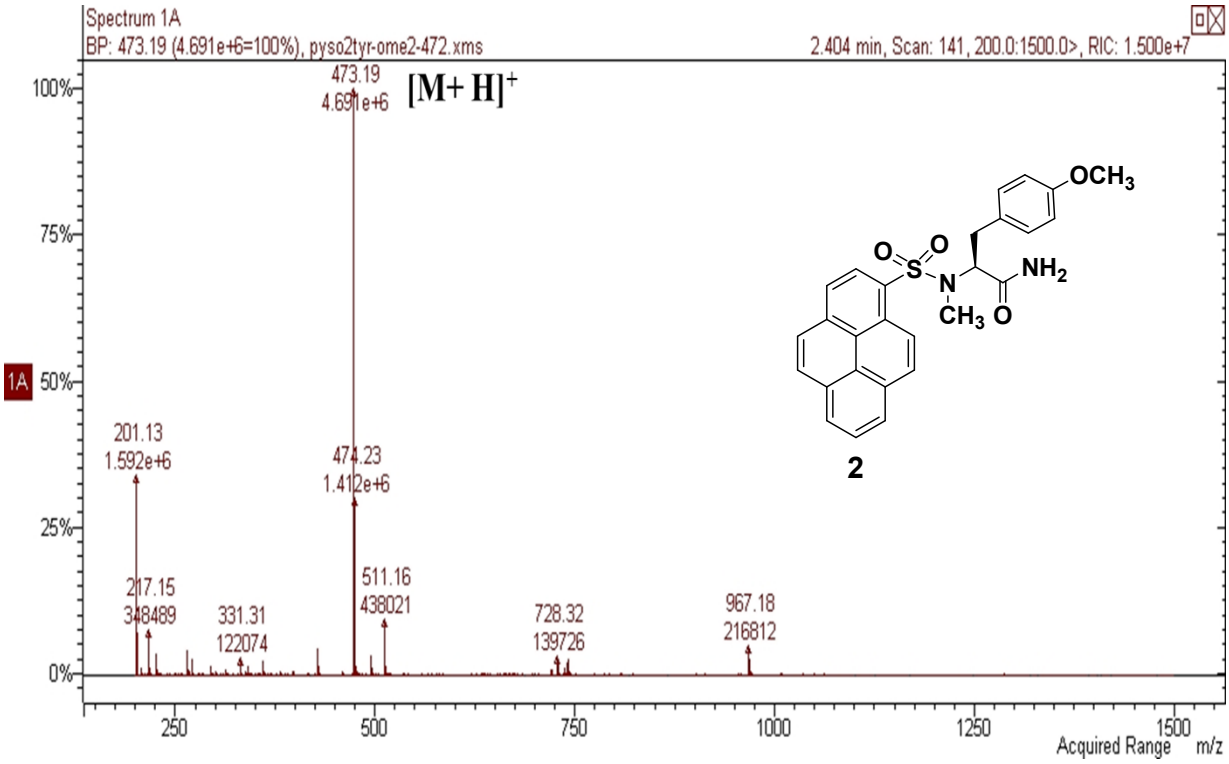

Fig. S9 ESI mass spectrum of **2**

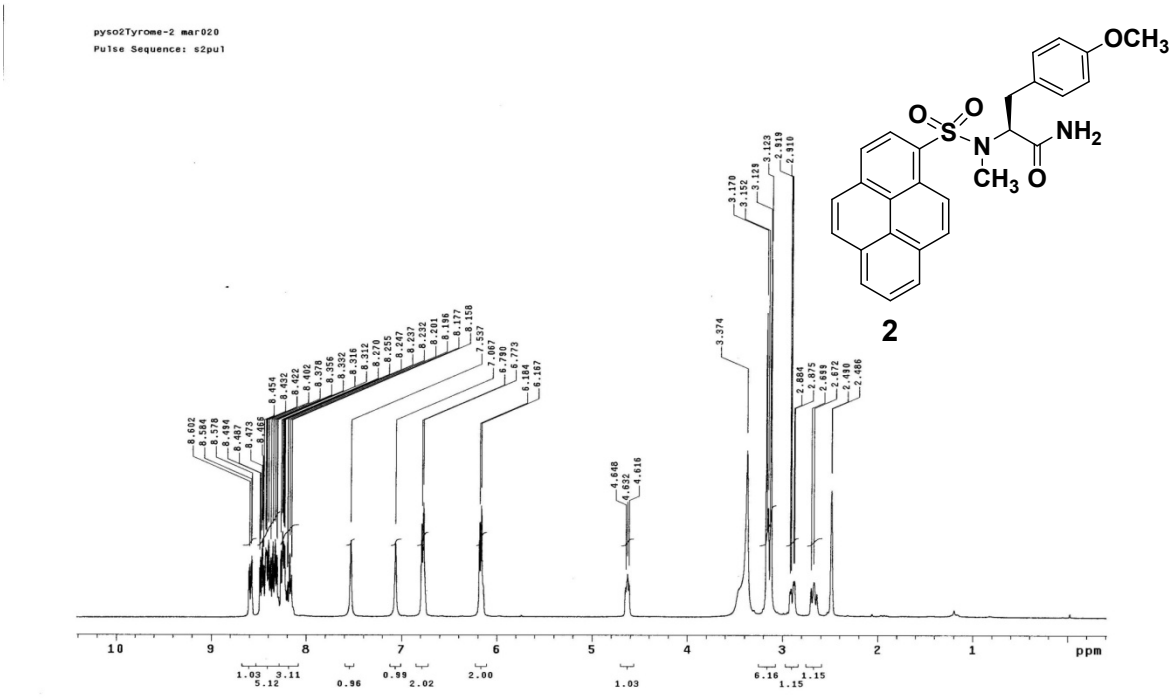

Fig. S10 ^{1}H NMR spectrum of compound **2**

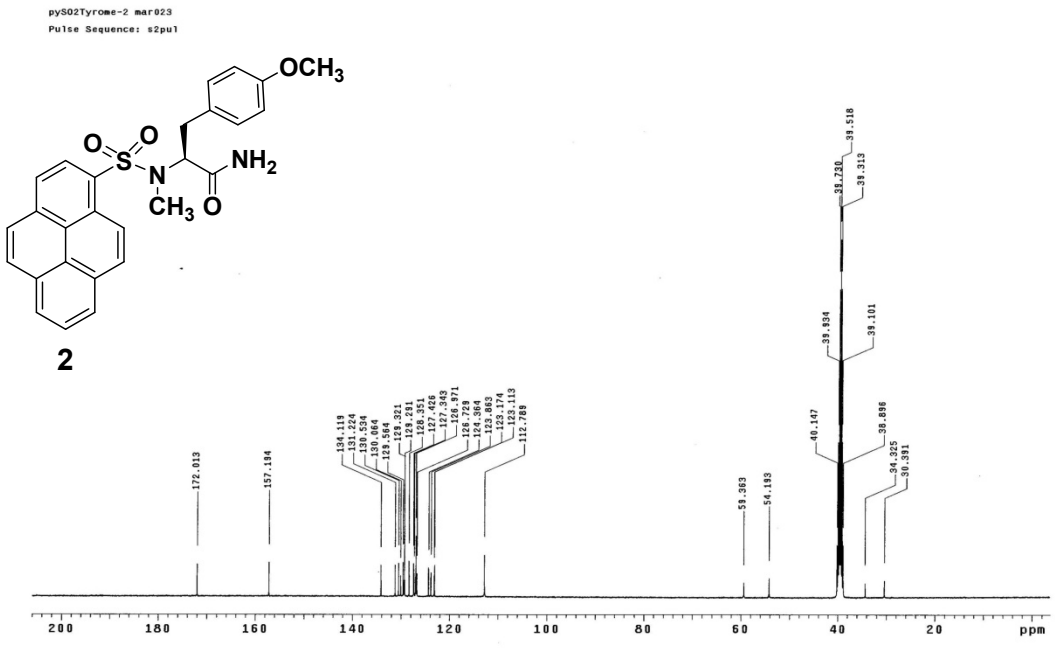

Fig. S11 ^{13}C NMR spectrum of compound **2**

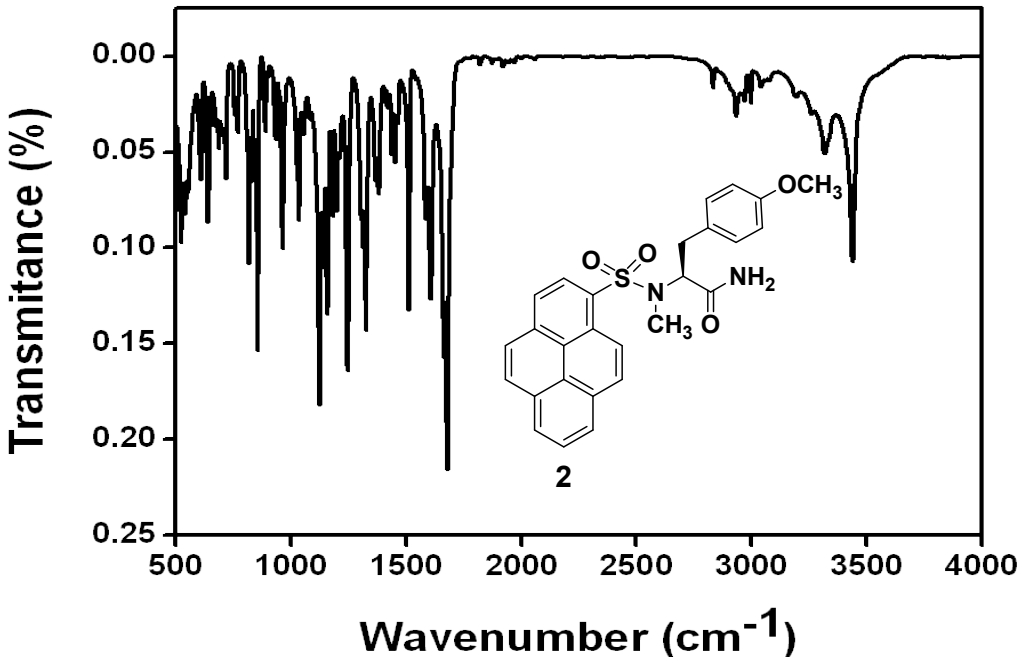

Fig. S12 IR spectrum of **2**

2) PYSO2-2 *with GLY (POS)*

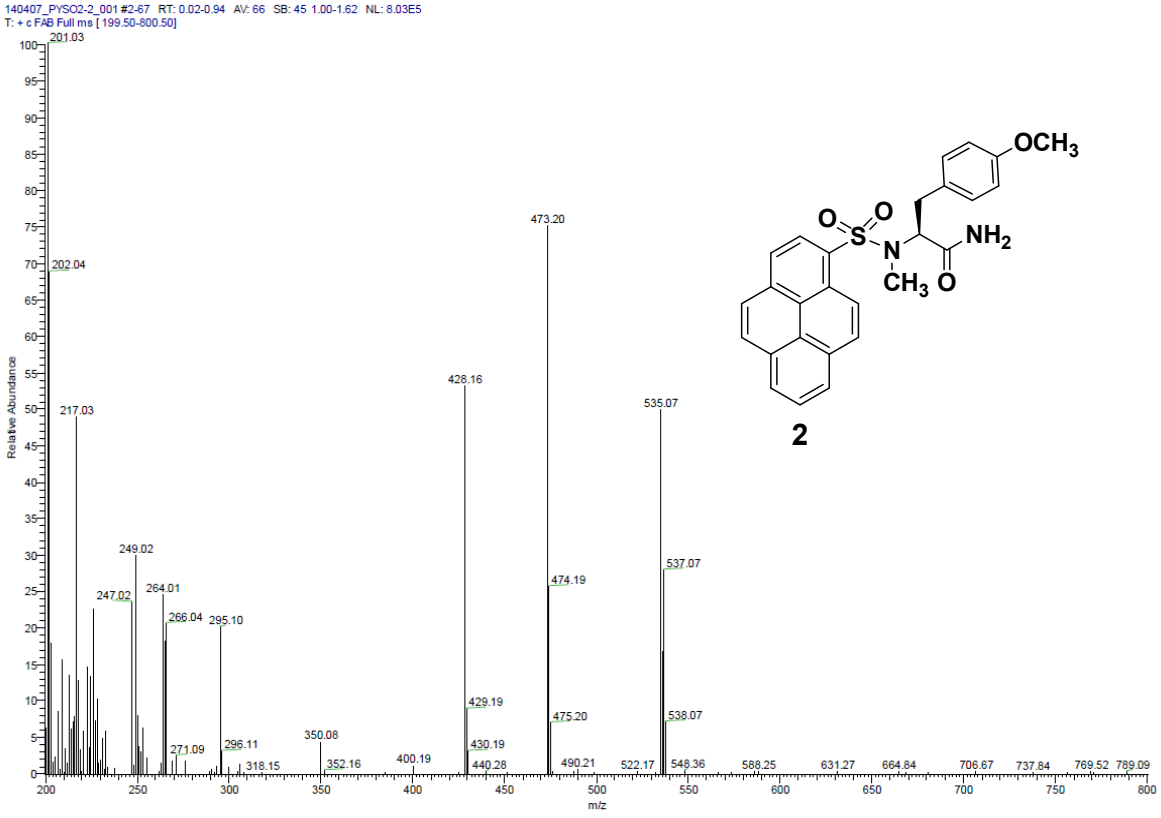

Fig. S13 HRMS-FAB mass spectrum of **2**

2) PYSO2-2 *with GLY (POS)*

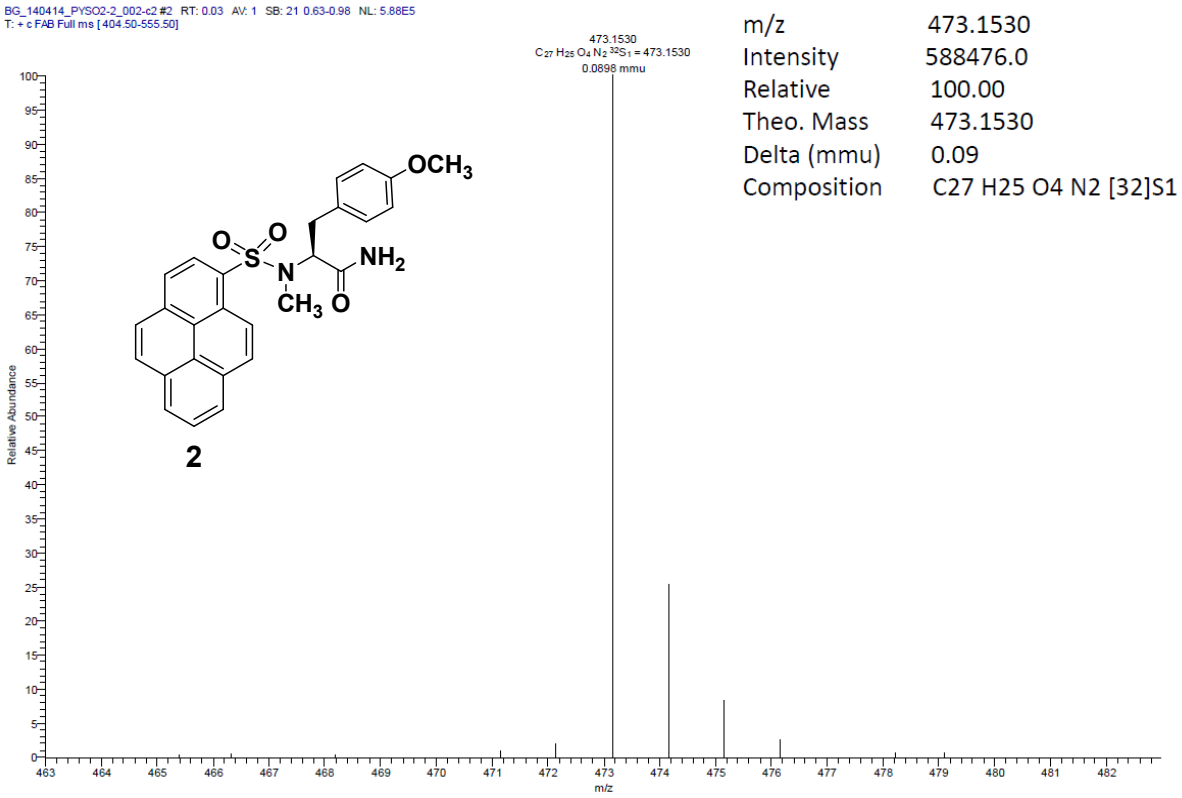

Fig. S14 HRMS-FAB elemental composition of **2**

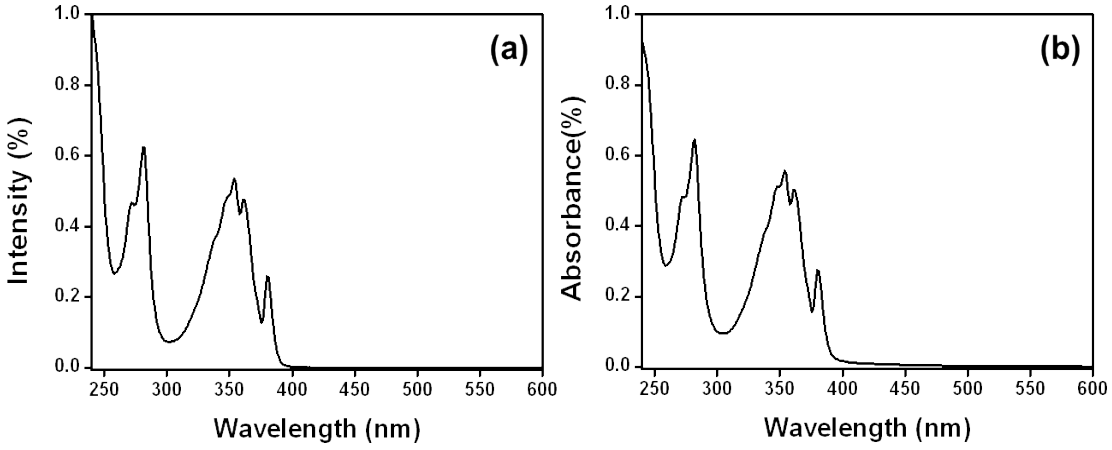

Fig. S15 UV-Visible absorption spectra of (a) **1** (40 μM) and (b) **2** (40 μM) in aqueous solution (H_2O/DMSO = 95:5, v/v, 10 mM HEPES at pH 7.4.

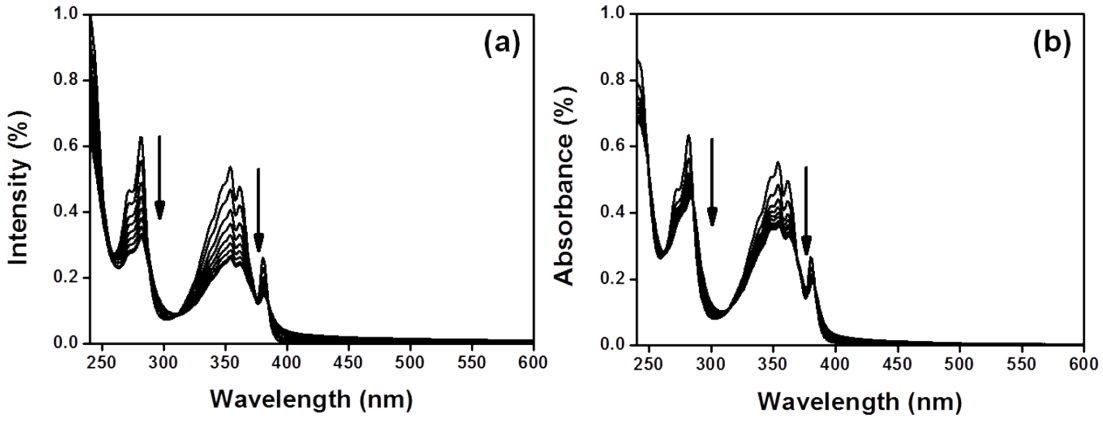

Fig. S16 UV−Visible absorption spectra of (a) **1** (40 μM) upon gradual addition of Hg(II) (0, 0.125, 0.250, 0.375, 0.500, 0.625, 0.75, 0.875, 1.00 and 1.125 equiv)and (b) **2** (40 μM) upon gradual addition of Hg(II) (0, 0.125, 0.250, 0.375, 0.500, 0.625, 0.75, 0.875, 1.00, 1.125 and 1.25 equiv) in aqueous solution (H_2O/DMSO, 95:5, v/v, 10 mM HEPES at pH 7.4).

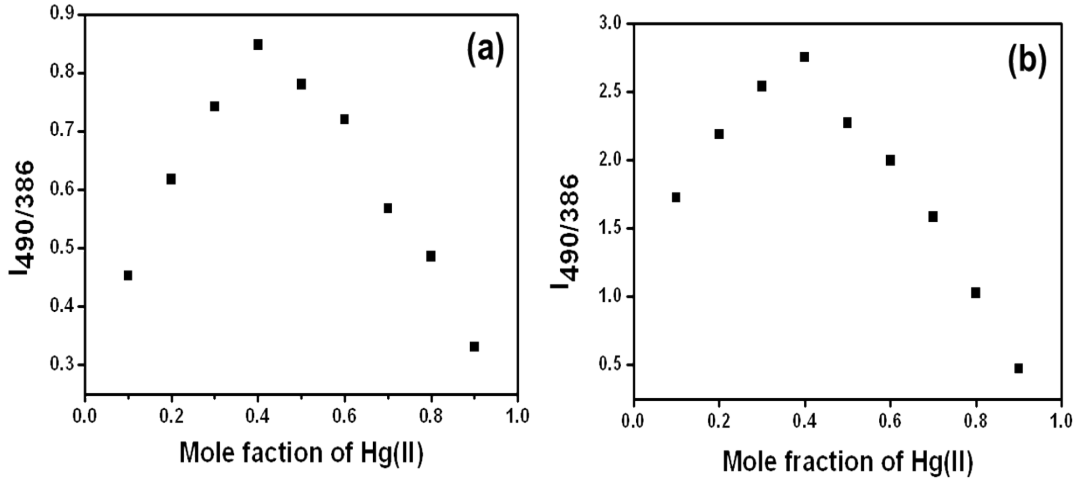

Fig. S17 A Job's plot analysis for (a) **1**, and (b) **2** with Hg(II).

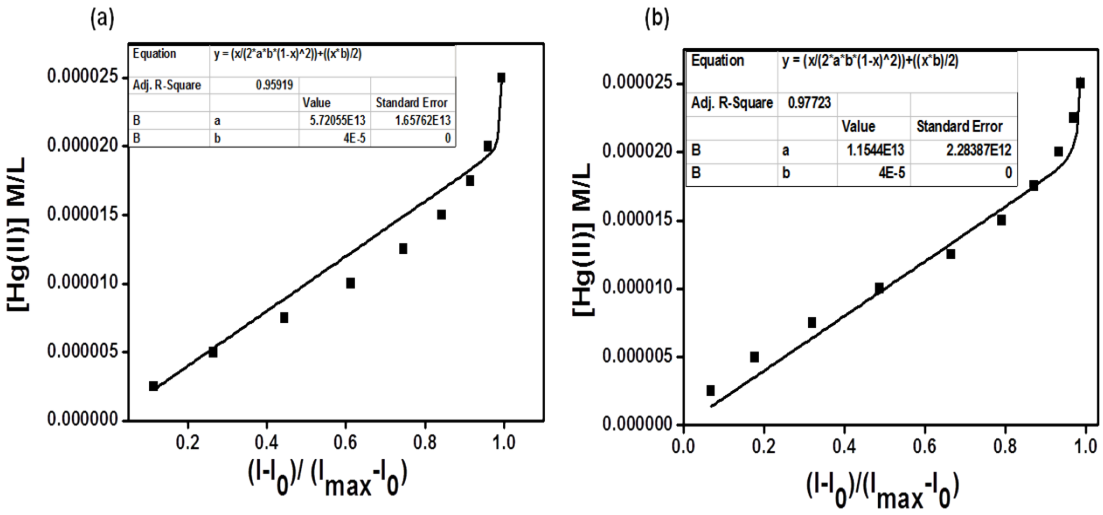

Fig. S18 Non-linear fitting of the fluorescence intensity change of (a) **1** at 490 nm *vs* concentration of Hg(II) (slit 15/5) (b) **2** at 486 nm *vs* concentration of Hg(II) (slit 15/6) in aqueous solution (H_2O/DMSO, 95:5, v/v, 10 mM HEPES at pH 7.4).

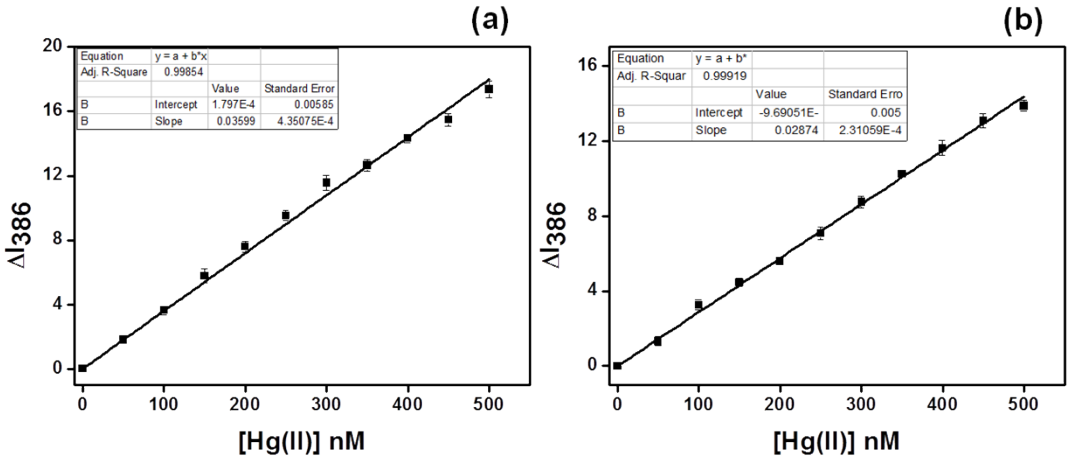

Fig. S19 Detection limit for (a) **1** and (b) **2** with Hg(II) (Intensity change at 386 nm) in aqueous solution (H_2O/DMSO = 95:5, v/v, 10 mM HEPES at pH 7.4; λ_{ex}= 353 nm, slit 15/6).

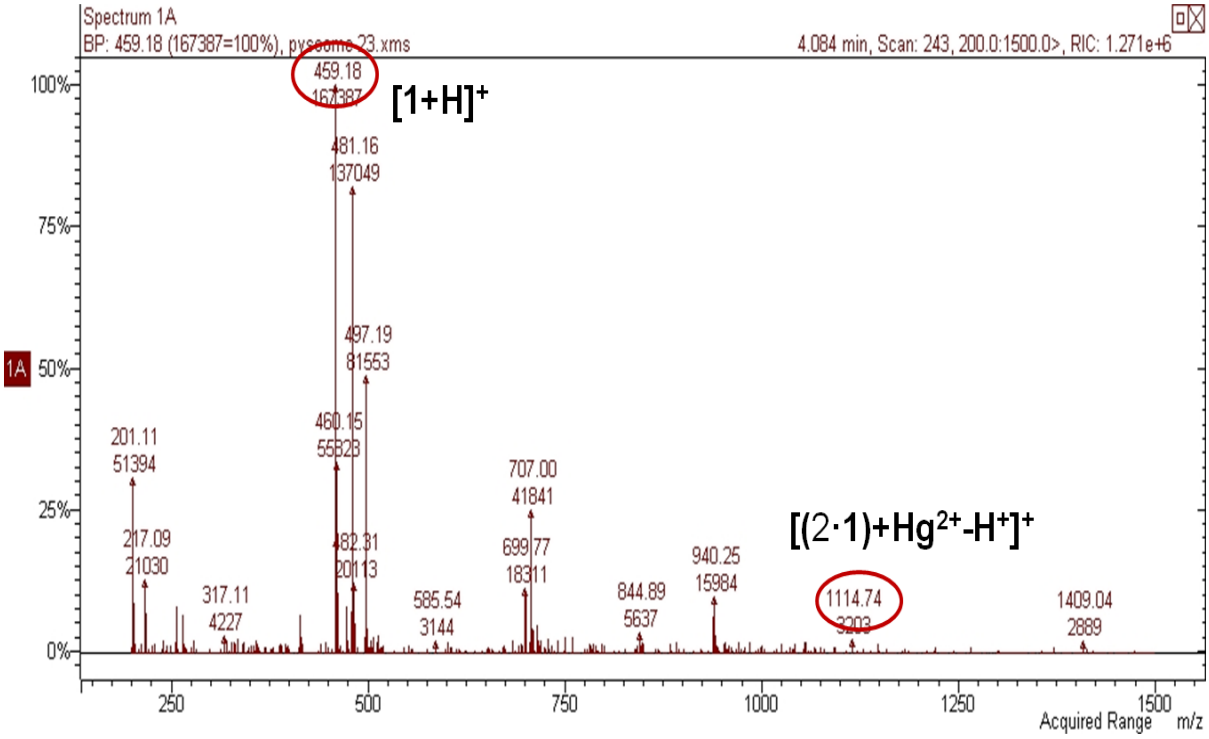

Fig. S20 ESI mass spectra of **1** (500 μM) in the presence of 1 equiv Hg(II) in aqueous solution (H_2O/ACN, 7:3, v/v).

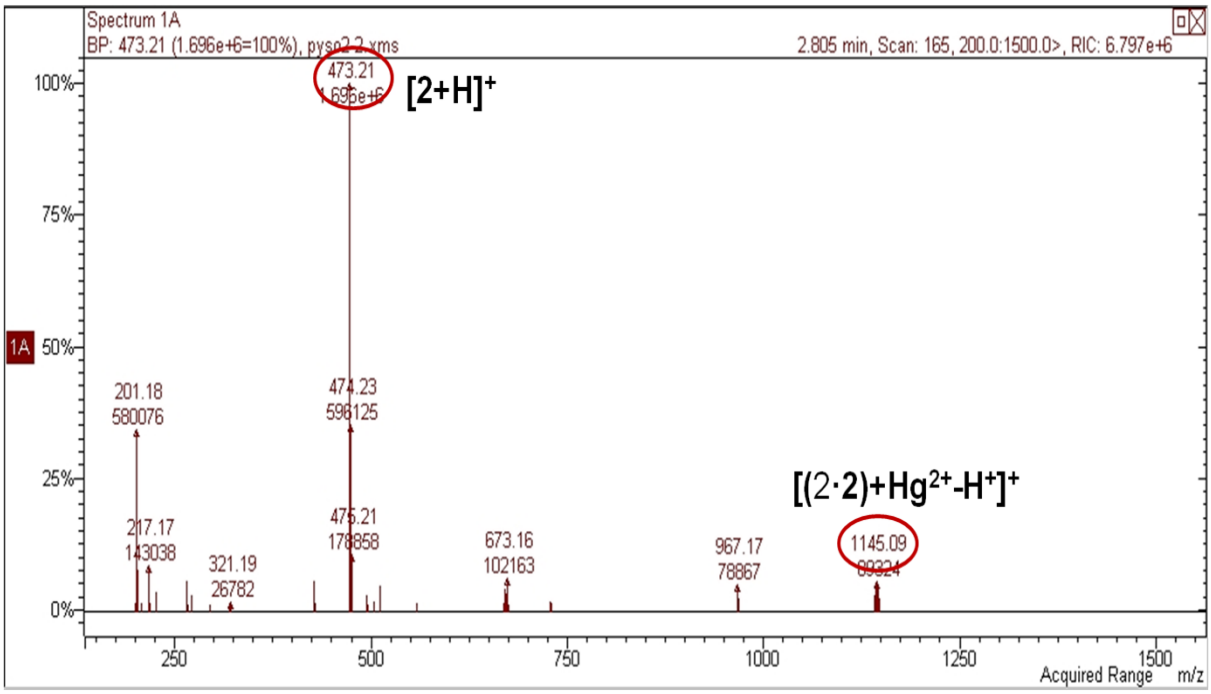

Fig. S21 ESI mass spectra of **1** (500 μM) in the presence of 1 equiv Hg(II) in aqueous solution (H_2O/ACN, 7:3, v/v).